Supplementary Information

Two dimensional Co(OH)$_2$ catalytic membrane for water purification: A highly green and facile

fabrication strategy and excellent water decontamination performance

Xiaoyu Zhao [a,b,c], Mei Long [a,b,c], Zhixing Li [a,b,c] and Zhenghua Zhang [a,b,c]*

[a.] Institute of Environmental Engineering & Nano-Technology, Tsinghua Shenzhen International

Graduate School, Tsinghua University, Shenzhen 518055, Guangdong, China

[b.] Guangdong Provincial Engineering Research Centre for Urban Water Recycling and Environmental

Safety, Tsinghua Shenzhen International Graduate School, Tsinghua University, Shenzhen, 518055,

Guangdong, China

[c.] School of Environment, Tsinghua University, Beijing 100084, China

Materials Horizons

Submitted November 2023

*Corresponding author: zhenghua.zhang@sz.tsinghua.edu.cn (Z.H. Zhang)

1. Experimental

1.1 Materials

The MCE substrate membrane (pore size = 0.2 μm) was purchased from Tianjin JINTENG Technology Co., Ltd. Potassium peroxymonosulfate (PMS, $KHSO_5$) was purchased from Titan Scientific, China. Cobalt nitrate hexahydrate ($Co(NO_3)_2.6H_2O$), 2-methylimidazole (2-MI), sulfuric acid (H_2SO_4, AR), sodium hydroxide (NaOH), sodium chloride (NaCl), sodium nitrate ($NaNO_3$), sodium sulfate (Na_2SO_4), sodium bicarbonate ($NaHCO_3$), tert-butyl alcohol (TBA), p-benzoquinone (p-BQ), 5,5-Dimethyl-pyrroline-N-oxide (DMPO), and 2,2,6,6-tetramethyl-4-piperidinol (TEMP) were obtained from Macklin, China. Tetracycline (TC), oxytetracycline (OTT), sulfamethoxazole (SMZ) and carbamazepine (CBZ) were supplied by Shanghai Yuanye Bio-Technology Co., Ltd. Methylene blue (MB, AR), rhodamine B (RhB, IND), bisphenol A (BPA), methanol (MeOH, ≥99.5%) and dimethyl sulfoxide (DMSO) were purchased from Aladdin Industrial Corporation. Ranitidine (RNTD) was received from Tokyo Chemical Industry Co. Ltd. Single layer graphene oxides (GO) aqueous dispersion was supplied by Hangzhou Gaoxi Technology Co. Ltd. Ultrapure water was obtained from a Milli-Q device and used to prepare solutions.

1.2 Catalyst synthesis and membrane fabrication

The $Co(OH)_2$ hexagonal nanosheets were fabricated via a green and facile method as depicted in Fig. 1(a). 145.5 mg $Co(NO_3)_2•6H_2O$ and 275 mg 2-MI were respectively dissolved in 30 mL pure water and quickly mixed together. The solution was kept under constant stirring for 24 hours, after which the solids were collected and washed via centrifugation (7500 rpm for 10 min) for 3 times. Then the products were dried in a vacuum oven at 60°C for hours. Composite catalysts ($Co(OH)_2$/rGO) were prepared with the similar protocol, during which the cobalt salt was dissolved in 20 mL water and 10 mL of GO solution (1 mg/g) was added at the same time. Pristine ZIF-67 was obtained through quickly mixing the precursor solution and keeping the mixture in undisturbed settlement for 1 hour.

To fabricate catalytic membrane, 6.3 mg prepared catalysts were thoroughly dispersed in 200 mL water via bath-sonication. Then the dispersion solution was rapidly filtered through a mixed cellulose ester (MCE) substrate (diameter = 5 cm, pore size = 0.22 μm) with assistance of a vacuum pump, and the catalysts could then be loaded on the membrane surface with an effective area of 12.56 cm^2. All the prepared membranes were dried at 60°C before use.

1.3 Characterization

Scanning electron microscopy (SEM) images were obtained from QUANTA 200 equipped with an energy dispersive spectroscopy (EDS). X-ray diffractions (XRD) of both catalyst powders and catalytic membranes were measured and recorded on Japan Ultima VI with Cu-$K\alpha$ radiation. The scanning rate was 5°/min and the scanning range was 5~90°. Brunauer-Emmett-Teller (BET) equation and the nitrogen adsorption technique (ASAP 2460) were adopted to acquire the specific surface area and pore size information of catalysts. The surface element chemical states of catalysts were characterized by X-ray photoelectron spectroscopy (XPS) on US Thermo Scientific K-Alpha. Raman analysis (WiTech alpha 300R) was used to obtain structure information of the composite materials. The detection of active species generated in the catalysis processes was performed on an electron paramagnetic resonance (EPR) spectroscopy (Bruker MS-5000). The RNTD degradation products were analyzed by liquid chromatography tandem mass spectrometry (LC-MS) on US Thermo Scientific Ultimate 3000 UHPLC-Q Exactive (Table S1). Inductively coupled plasma tandem mass spectrometry (ICP-MS) analysis was performed on Agilent 7700 to acquire the concentration of leached cobalt ions in membrane filtrates.

1.4 Techniques and methods

1.4.1 Pollutant degradation in batch and membrane systems

The RNTD degradation batch reaction was carried out in a 150 mL beaker. The batch solution contained 5 mg/L RNTD and certain amounts of catalysts. 0.2 mM PMS was added to initiate the AOP reactions. Before the addition of PMS, the pH value of the solution would be tested and adjusted by 0.1 M H_2SO_4

and 0.1 M NaOH. At regular time intervals, 1.5 mL of the reaction solution was extracted and filtered through a 0.22 μm membrane before measurement. The membrane catalytic performance was tested on a dead-end filtration unit with no external pressure applied. 5 mg/L RNTD and 0.2 mM PMS solutions were mixed together as the feed. The filtrate was collected at certain time intervals.

The RNTD content was determined by the solution ultraviolet (UV) absorbance at 314 nm. Besides, the total organic carbon (TOC) of the solution sample was also measured on a TOC analyzer to evaluate the system mineralization efficiency. The membrane flux was calculated according to Eq. (1), where J represents the membrane flux (LMH), V is the membrane filtration volume (L), A is the membrane effective area (m^2), and T is the filtration time (h).

$$J = \frac{V}{A \times T}$$

(1)

Additionally, the kinetic constants (k) of different systems were calculated using a pseudo-first-order reaction model (Eq. (2)), where C_0 and C_t respectively represent the initial RNTD content and that of the solution sample collected at certain time point (t).

$$\ln\left(\frac{C_t}{C_0}\right) = -k \times t$$

(2)

1.4.2 PMS decomposition rate

The PMS decomposition rate was assessed with a UV spectrophotometer. Before the measurement, reserve solution containing 100 g/L KI and 5 g/L $NaHCO_3$ was prepared. During the degradation tests, 0.2 mL reaction solution was collected and mixed with 20 mL of the reserve solution, which was then kept for about 30 min. The absorbance at 352 nm of the mixed solution was measured, and the corresponding PMS degradation rate was calculated as follow:

$$R = \frac{A_0 - A_t}{A_0} \times 100\%$$

(3)

In the Eq. (3), R represents the PMS decomposition rate, A_0 is the initial absorbance of 0.2 mM PMS, and A_t is the absorbance of sample solutions collected at certain time point.

1.4.3 Interference and quenching tests

To evaluate the universality and adaptivity of the fabricated catalytic membrane, ions (Cl^-, SO_4^{2-}, NO_3^- and HCO_3^-) and humic acid were introduced into the reaction systems. Certain amounts of interference substances were added into the feed solution before filtered through the catalytic membrane.

Quenching experiments were performed to verify the generated reactive oxidative species (ROS) in the system and speculate their contribution to the pollutant degradation. TBA (90 mM) was used as quencher for •OH. MeOH (90 mM) could quench both •OH and $SO_4^{•-}$. TEMP (1 mM) was adopted to quench $^1O_2$. The $O_2^{•-}$ was quenched by pBQ (1 mM). DMSO (2 mM) was applied to detect high-valent metal species. The quenchers were added into the mixture of RNTD and PMS before the catalytic filtration process. Particularly, all these membrane tests with additional chemicals were carried out after an hour of degradation reaction so as to guarantee the stabilized catalytic performance of the membrane.

### 1.4.4 Biotoxicity analysis of degradation products

The biotoxicity of RNTD and its degradation products were assessed by the ECOSAR program based on the principle of quantitative structure-activity relationship[1]. The chemical structures of degradation intermediates were obtained via the LC-MS analysis. The product toxicity was predicted and profiled as the lowest detrimentally effective concentration towards three aquatic species (fish, daphnid and green algae). Specifically, the acute toxicity can be reflected by the pollutant concentration causing 50% death (LC_{50}) of fish (after 96 h exposure) and daphnid (after 48 h exposure), and the pollutant concentration

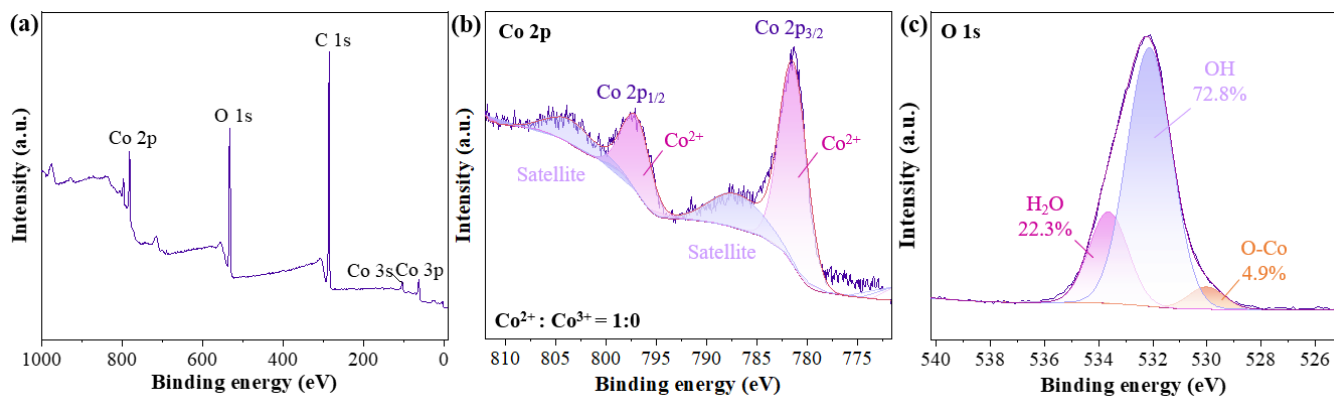causing 50% growth inhibition (EC_{50}) of green algae (after 96 h exposure).

2. Figures
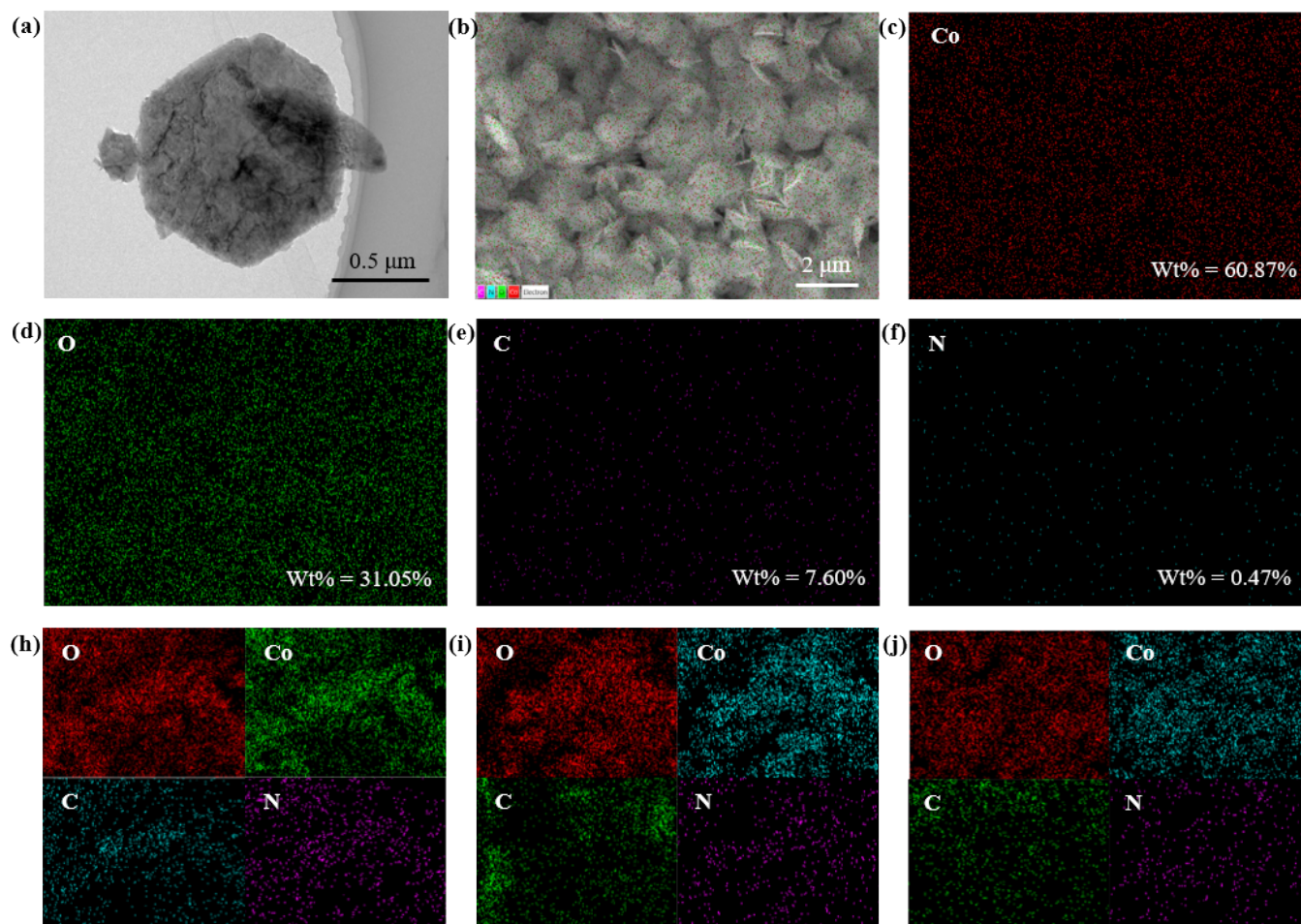
Fig. S1. (a) The TEM image of the prepared Co(OH)$_2$ nanosheets. The EDS mapping results of products collected after different stirring period: **(b–f)** 24-hour stirring; **(h)** 3-hour stirring; **(i)** 5-hour stirring; **(j)** 10-hour stirring.
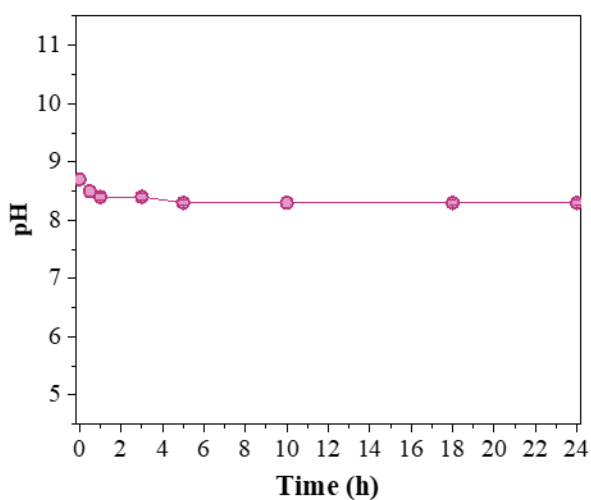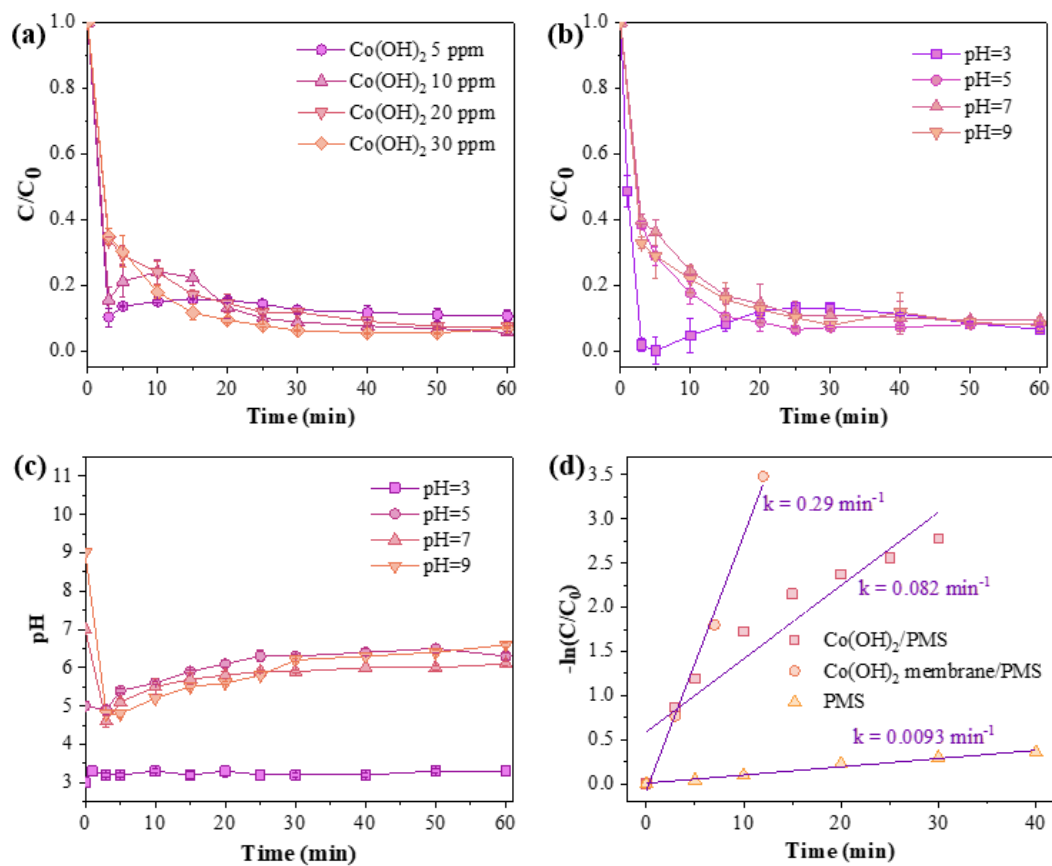

**Fig. S2.** The pH variation during the Co(OH)$_2$ preparation process.

Fig. S3. (a) Co(OH)$_2$ membrane XPS survey spectrum and its high-resolution spectra of **(b)** Co 2p, **(c)** O 1s.
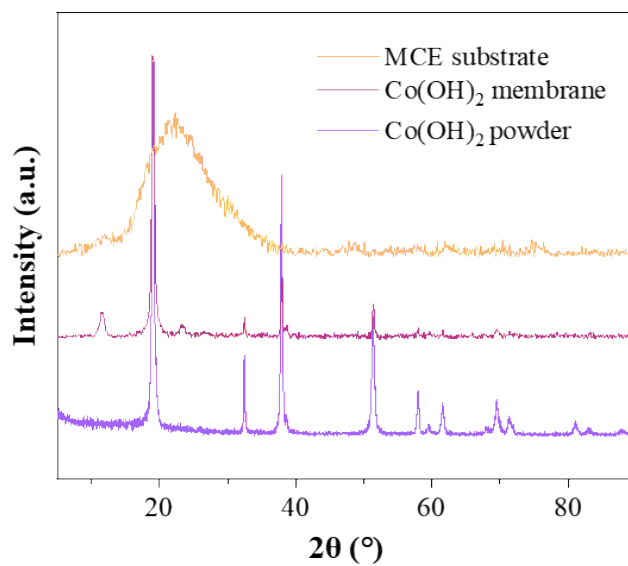

Fig. S4. The XRD patterns of MCE substrate, Co(OH)$_2$ catalyst powder and Co(OH)$_2$ catalytic membrane.

**Fig. S5.** Catalytic AOP performance: Co(OH)$_2$ batch reaction with **(a)** different catalyst dosages and **(b)** initial pH values. **(c)** The pH variation during the Co(OH)$_2$ batch system catalysis reaction process under different initial pH values. **(d)** The pseudo-first-order reaction rate constants of different systems.
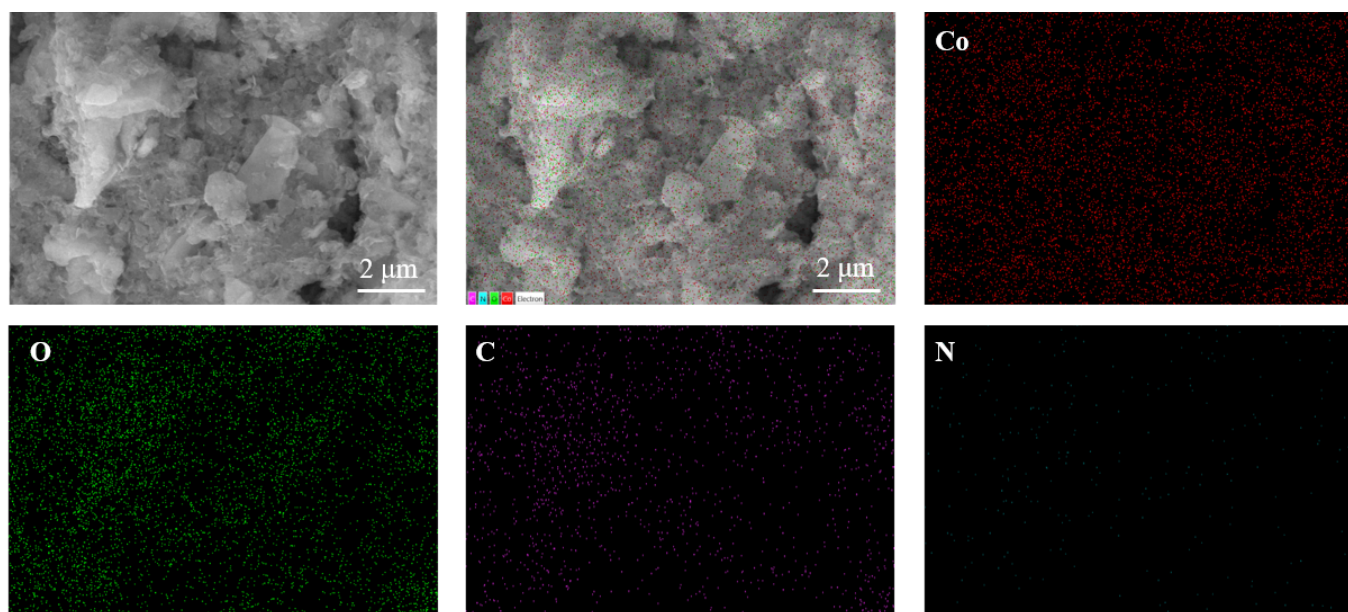
Fig. S6. The EDS mapping results of Co(OH)$_2$/rGO composites.
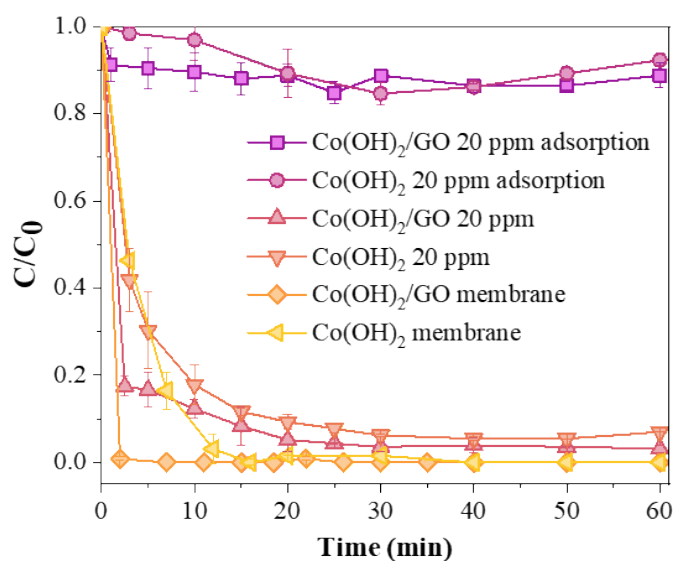
Fig. S7. The comparison of catalytic performance and adsorption effects in $Co(OH)_2$ and $Co(OH)_2/rGO$ systems. (Conditions: [RNTD] = 5 mg/L, [PMS] = 0.2 mM, initial pH = 5.0±0.1, temperature = 25°C.)
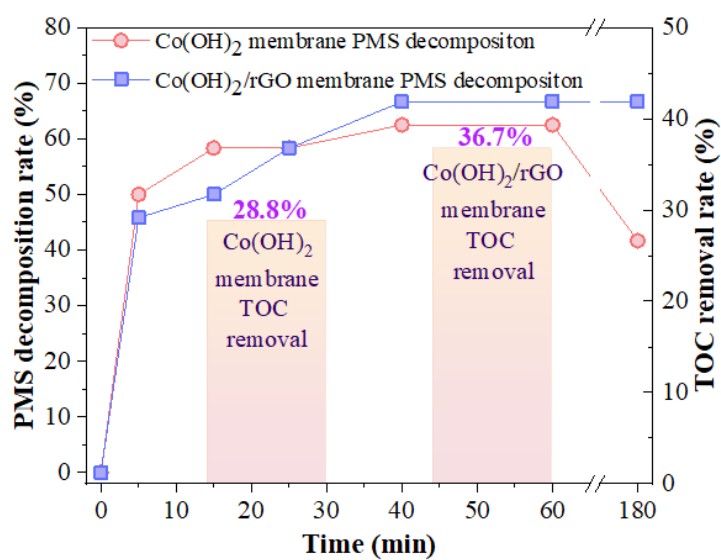
Fig. S8. TOC removal efficiency and PMS decomposition rate of catalytic membranes.
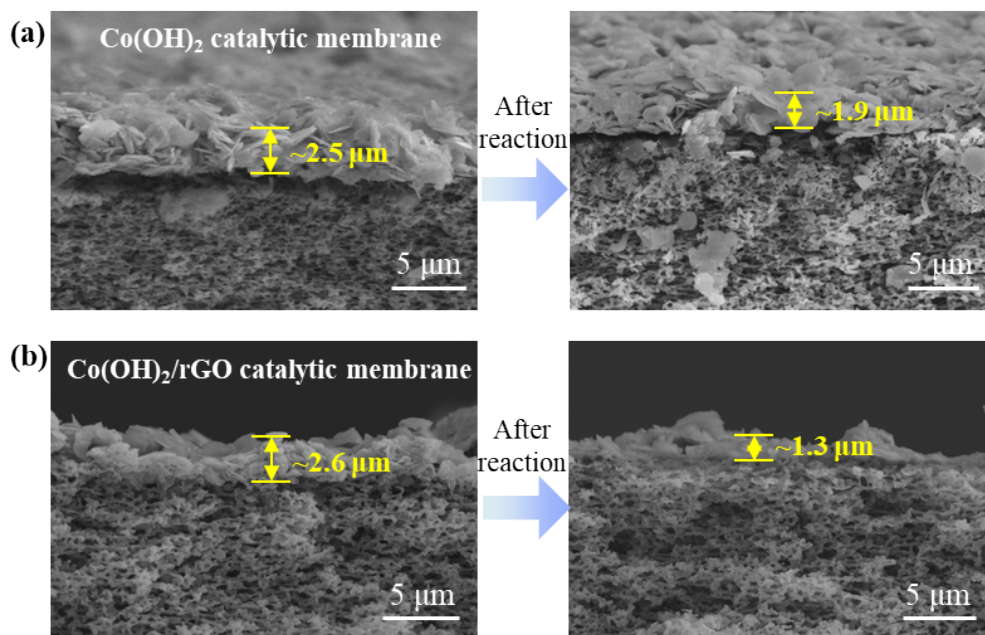
Fig. S9. The SEM morphology comparison of membranes before and after the long-term reaction.
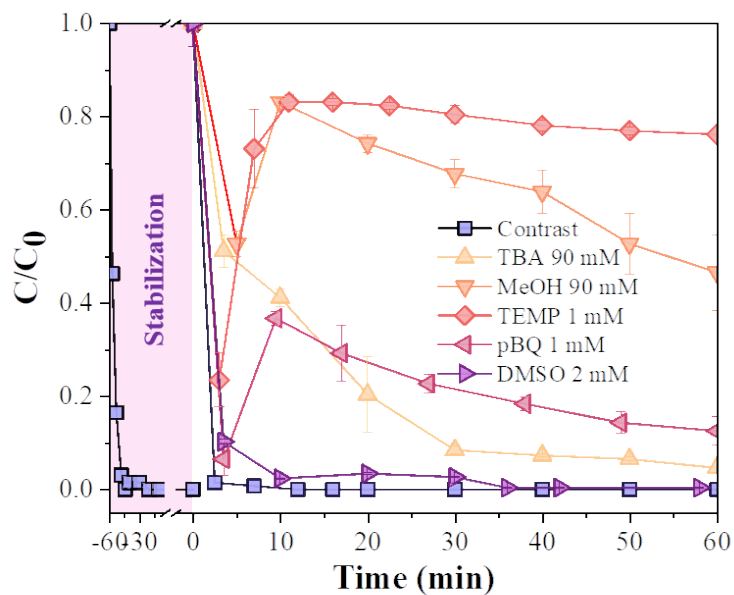
Fig. S10. The quenching experiment results of the Co(OH)$_2$ catalytic membrane.
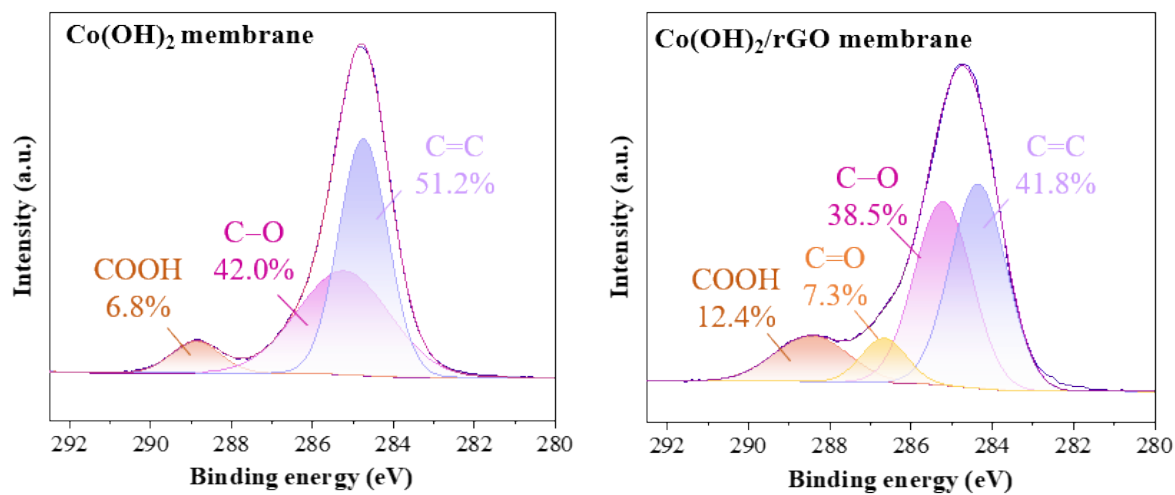
Fig. S11. The high resolution C 1s XPS spectra of $Co(OH)_2$ and $Co(OH)_2/rGO$ membranes.

Fig. S12. Electrochemical impedance spectroscopy test results of $Co(OH)_2$ and $Co(OH)_2/rGO$ catalysts.

3. Tables

Table S1. Operating condition parameters of the LC-MS measurement.

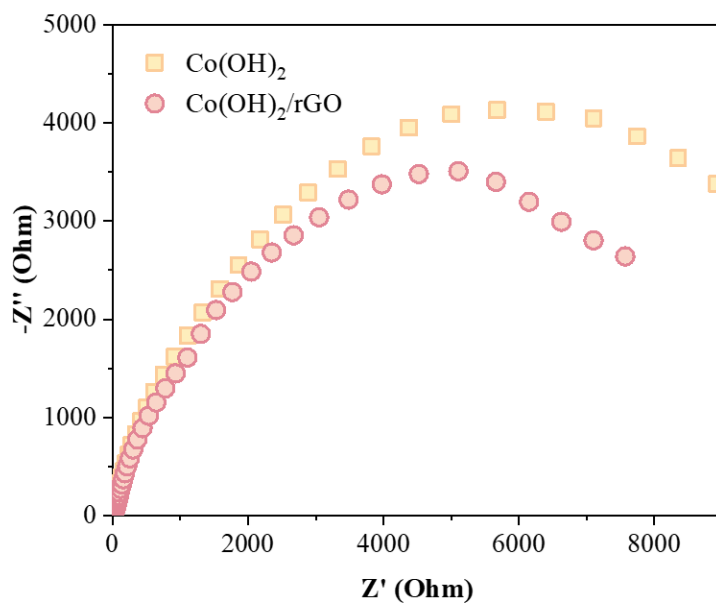| LC operating conditions	
Chromatographic column	Eclipse Plus C18 100mm×4.6mm, 3.5μm
Column temperature	30°C
Sample injection	20.0μL
Effluent A	0.1% Formic acid solution
Effluent B	Methanol
MS operating conditions	
Sheath gas rate	40 arb
Auxiliary gas rate	10 arb
Sprat voltage	Positive ion 3.0kV
Capillary temperature	320°C
Auxiliary gas temperature	300°C
Scanning mode	Fullms/dd ms2 top10
Scanning range	50~400 m/z
Collision voltage	NCE10, 20, 30

Table S2. Specific water quality parameters for different real water matrices.

Samples	Tap water	Lake water[a]
pH	7.04	6.91
COD (mg/L)	$-$[b]	<15
NH_3 (mg/L)	$-$	0.09
NO_3^- (mg/L)	1.40	0.11
PO_4^{3-} (mg/L)	$-$	<0.01
Cl^- (mg/L)	15.90	4.19
CO_3^{2-} (mg/L)	$-$	16.90
Conductivity (μS/cm)	182.80	47.20

[a]Lake water was collected from Tsinghua SIGS campus in Shenzhen University Town.

[b]" $-$ " means that the parameter was undetected or the concentration of the target parameter was below the detection limit.

Table S3. The comparison of reusability or long-term stability of heterogeneous catalysts and catalytic AOP membranes.

Batch reaction catalysts			
Materials	Repeated cycles	Total reaction time	Reference
Cu_xNi_yCo-LDH nanosheets/GO	5	200 min	[2]
Cobalt silicate hydroxide	5	100 min	[3]
CoFe-LDH	3	36 min	[4]
CuCo-LDH	10	300 min	[5]
CoOOH/GO hydrogel	10	50 min	[6]
$Co(OH)_2$/nickel foam	6	42 min	[7]
$Co(OH)_2/WO_3$	5	100 min	[8]
CuAl-LDH	6	24 min	[9]
Co/N-doped carbon composites	5	300 min	[10]
Catalytic AOP membranes			
Loaded catalysts	Reaction time		Reference
Co/g-C_3N_4	100 h		[11]
Co-TiO_x nanosheets	100 h		[12]
Co-Al oxides	29 h		[13]
Co.Cu oxides	120 h		[14]
Fe-doped $CoTiO_3/SiO_2$	300 min		[15]
$CoFe_2O_4/Mn_3O_4$@g- C_3N_4	150 min		[16]
$Co(OH)_2$	15 h		this work
$Co(OH)_2$/GO	165 h		this work

Table S4. The catalysis performance comparison of different cobalt-containing catalytic membranes.

Catalyst	Substrate	Filtration condition	Flux (LMH/bar)	Oxidant	Pollutant	Removal efficiency (%)	Ref.
Co@g-C_3N_4	CA[a]	Vacuum-assisted	224	0.16 mM PMS	5 mg/L RNTD[b]	100	[11]
Co_3O_4 nanosheets	CA	Vacuum-assisted	175	0.16 mM PMS	5 mg/L RNTD	100	[17]
Co.Cu oxides	PVDF[c]	Vacuum-assisted	357	0.16 mM PMS	5 mg/L RNTD	100	[14]
Fe-doped $CoTiO_3$	SiO_2 fibers	Gravity-driven	300	1 mM PMS	10 mg/L Nimesulide	96.3	[15]
$CoFe_2O_4/Mn_3O_4$@g-C_3N_4	PVDF	Gravity-driven	300	0.75 mM PMS	10 mg/L Norfloxacin	94.5	[16]
MnO/Co@SiO_2	Carbon fibers	Gravity-driven	752	500 mg/L PMS	20 mg/L MB[d]	99.5	[18]
Co-Al oxides	PVDF	Gravity-driven	75	30.4 mg/L PMS	1 mg/L RNTD	94	[19]
Co_3O_4/C@SiO_2	PVP[e]	Vacuum-assisted	229	100 mg/L PMS	10 mg/L BPA[f]	95	[20]
$CoFe_2O_4$	Ceramic	Vacuum-assisted	236	100 mg/L PMS	10 mg/L SMX[g]	98	[21]
Co-TPL[h]	PVDF	Vacuum-assisted	500	10 mM PMS	2 μM BPA	90	[22]
Co/C	PAN[i]	Vacuum-assisted	140	30.4 mg/L PMS	10 mg/L SMX	90	[23]
$Co(OH)_2$	MCE[j]	Gravity-driven	560	0.2 mM PMS	5 mg/L RNTD	100	This work
$Co(OH)_2$/GO	MCE	Gravity-driven	250	0.2 mM PMS	5 mg/L RNTD	100	This work

[a]CA: Cellulose acetate; [b]RNTD: Ranitidine; [c]PVDF: Polyvinylidene fluoride; [d]MB: Methylene blue; [e]PVP: Polyvinylpyrrolidone; [f]BPA: Bisphenol A; [g]SMX: Sulfamethoxazole; [h]TPL: Tetrapyridomacrocyclic; [i]PAN: Polyacrylonitrile; [j]MCE: Mixed cellulose esters.

Table S5. The cobalt leaching concentration in filtrates of different membrane systems.

Batch reaction		
Reaction time	$Co(OH)_2$ powders	$Co(OH)_2$/rGO powders
1 h	3.30 mg/L	2.75 mg/L
Membrane system reaction		
Reaction time	$Co(OH)_2$ membrane	$Co(OH)_2$/rGO membrane
1 h	2.02 mg/L	1.56 mg/L
5 h	0.19 mg/L	0.17 mg/L
10 h	0.16 mg/L	0.06 mg/L
100 h	–[a]	3.10 μg/L

[b]" –" here means that the filtrate sample after 100-hour reaction in $Co(OH)_2$ membrane/PMS system was not collected because that the $Co(OH)_2$ membrane was already disabled after reactions lasting for more than 15 hours.

Table S6. The toxicity classification criteria regulated by the Globally Harmonized System of Classification and Labelling of Chemicals (2021).

Concentration range (mg/L)	Toxicity category
< 1	Extremely toxic
1~10	Toxic
10~100	Harmful
>100	Harmless

Table S7. The ECOSAR assessment results of RNTD and its degradation products (mg/L).

Chemicals	Fish LC$_{50}$ (96 h)	Daphnid LC$_{50}$ (48 h)	Green algae EC$_{50}$ (48 h)
RNTD	797.93	78	95.29
P7 (m/z = 227)	2096.09	185.55	275.83
P6 (m/z = 192)	2440.48	210.88	328.83
P5 (m/z = 185)	1531	136.62	199.89
P4 (m/z = 163)	7208.37	565.48	1067.57
P3 (m/z = 118)	11211.91	830.76	1755.84
P2 (m/z = 107)	55518.32	23648.6	5367.47
P1 (m/z = 89)	1451.86	123.03	199.4

4. References

[1] G. Chen, H. Wang, W. Dong, W. Ding, F. Wang, Z. Zhao, Y. Huang, The overlooked role of Co(OH)(2) in Co3O4 activated PMS system: Suppression of Co2+ leaching and enhanced degradation performance of antibiotics with rGO, Sep. Purif. Technol. 304 (2023). https://doi.org/10.1016/j.seppur.2022.122203.

[2] Z. Wu, Y. Gu, S. Xin, L. Lu, Z. Huang, M. Li, Y. Cui, R. Fu, S. Wang, CuxNiyCo-LDH nanosheets on graphene oxide: An efficient and stable Fenton-like catalyst for dual-mechanism degradation of tetracycline, Chem. Eng. J. 434 (2022). https://doi.org/10.1016/j.cej.2022.134574.

[3] P. Shao, J. Tian, X. Duan, Y. Yang, W. Shi, X. Luo, F. Cui, S. Luo, S. Wang, Cobalt silicate hydroxide nanosheets in hierarchical hollow architecture with maximized cobalt active site for catalytic oxidation, Chem. Eng. J. 359 (2019) 79–87. https://doi.org/10.1016/j.cej.2018.11.121.

[4] Z. Yang, X. Li, Y. Huang, Y. Chen, A. Wang, Y. Wang, C. Li, Z. Hu, K. Yan, Facile synthesis of cobalt-iron layered double hydroxides nanosheets for direct activation of peroxymonosulfate (PMS) during degradation of fluoroquinolones antibiotics, J. Clean. Prod. 310 (2021). https://doi.org/10.1016/j.jclepro.2021.127584.

[5] R. Guo, L. Nengzi, Y. Chen, Y. Li, X. Zhang, X. Cheng, Efficient degradation of sulfamethoxazole by CuCo LDH and LDH@fibers composite membrane activating peroxymonosulfate, Chem. Eng. J. 398 (2020). https://doi.org/10.1016/j.cej.2020.125676.

[6] Q. Yi, J. Tan, W. Liu, H. Lu, M. Xing, J. Zhang, Peroxymonosulfate activation by three-dimensional cobalt hydroxide/graphene oxide hydrogel for wastewater treatment through an automated process, Chem. Eng. J. 400 (2020). https://doi.org/10.1016/j.cej.2020.125965.

[7] R. Yuan, M. Jiang, S. Gao, Z. Wang, H. Wang, G. Boczkaj, Z. Liu, J. Ma, Z. Li, 3D mesoporous alpha-Co(OH)(2) nanosheets electrodeposited on nickel foam: A new generation of macroscopic cobalt-based hybrid for peroxymonosulfate activation, Chem. Eng. J. 380 (2020). https://doi.org/10.1016/j.cej.2019.122447.

[8] W. Zhang, J. Liu, J. Tan, H. Yu, X. Liu, Facile route for fabricating Co(OH)(2)@WO3 microspheres from scheelite and its environmental application for high-performance peroxymonosulfate activation, J. Clean. Prod. 340 (2022). https://doi.org/10.1016/j.jclepro.2022.130714.

[9] H. Zeng, H. Zhu, J. Deng, Z. Shi, H. Zhang, X. Li, L. Deng, New insight into peroxymonosulfate activation by CoAl-LDH derived CoOOH: Oxygen vacancies rather than Co species redox pairs induced process, Chem. Eng. J. 442 (2022). https://doi.org/10.1016/j.cej.2022.136251.

[10] Y. Xue, N.N.T. Pham, G. Nam, J. Choi, Y.-Y. Ahn, H. Lee, J. Jung, S.-G. Lee, J. Lee, Persulfate activation by ZIF-67-derived cobalt/nitrogen-doped carbon composites: Kinetics and mechanisms dependent on persulfate precursor, Chem. Eng. J. 408 (2021). https://doi.org/10.1016/j.cej.2020.127305.

[11] W. Zhang, S. Zhang, C. Meng, Z. Zhang, Nanoconfined catalytic membranes assembled by cobalt-functionalized graphitic carbon nitride nanosheets for rapid degradation of pollutants, Appl. Catal. B Environ. 322 (2023) 122098. https://doi.org/10.1016/j.apcatb.2022.122098.

[12] C. Meng, B. Ding, S. Zhang, L. Cui, K.K. Ostrikov, Z. Huang, B. Yang, J.-H. Kim, Z. Zhang, Angstrom-confined catalytic water purification within Co-TiOx laminar membrane nanochannels, Nat. Commun. 13 (2022). https://doi.org/10.1038/s41467-022-31807-1.

[13] M.B. Asif, H. Kang, Z. Zhang, Gravity-driven layered double hydroxide nanosheet membrane activated peroxymonosulfate system for micropollutant degradation, J. Hazard. Mater. 425 (2022). https://doi.org/10.1016/j.jhazmat.2021.127988.

[14] C. Meng, Z. Wang, W. Zhang, L. Cui, B. Yang, H. Xie, Z. Zhang, Laminar membranes assembled by ultrathin cobalt-copper oxide nanosheets for nanoconfined catalytic degradation of contaminants, Chem. Eng. J. 449 (2022) 137811. https://doi.org/10.1016/j.cej.2022.137811.

[15] J. Wei, J. Bi, L. Zhang, D. Han, J. Gong, Gravity-driven Fe-doped CoTiO3/SiO2 fiber membrane with open catalytic network: Activation of peroxymonosulfate and efficient pollutants removal, Sep. Purif. Technol. 280 (2022). https://doi.org/10.1016/j.seppur.2021.119975.

[16] B. Chen, J. Wang, R. Li, H. Lin, B. Li, L. Shen, Y. Xu, M. Zhang, Fabrication of CoFe2O4/Mn3O4 decorated ultrathin graphitic carbon nitride nanosheets membrane for persistent organic pollutants removal: Synergistic performance and mechanisms, Sep. Purif. Technol. 309 (2023). https://doi.org/10.1016/j.seppur.2022.123076.

[17] Z. Wang, C. Meng, W. Zhang, S. Zhang, B. Yang, Z. Zhang, Honeycomb-like holey Co3O4 membrane triggered peroxymonosulfate activation for rapid degradation of organic contaminants, Sci. TOTAL Environ. 814 (2022). https://doi.org/10.1016/j.scitotenv.2021.152698.

[18] Z. Zhu, L. Zhong, Z. Zhang, H. Li, W. Shi, F. Cui, W. Wang, Gravity driven ultrafast removal of organic contaminants across catalytic superwetting membranes, J. Mater. Chem. A. 5 (2017) 25266–25275. https://doi.org/10.1039/c7ta08529j.

[19] M.B. Asif, H. Kang, Z. Zhang, Assembling CoAl-layered metal oxide into the gravity-driven catalytic membrane for Fenton-like catalytic degradation of pharmaceuticals and personal care products, Chem. Eng. J. 463 (2023). https://doi.org/10.1016/j.cej.2023.142340.

[20] J. Xie, Z. Liao, M. Zhang, L. Ni, J. Qi, C. Wang, X. Sun, L. Wang, S. Wang, J. Li, Sequential Ultrafiltration-Catalysis Membrane for Excellent Removal of Multiple Pollutants in Water, Environ. Sci. Technol. 55 (2021) 2652–2661. https://doi.org/10.1021/acs.est.0c07418.

[21] Y. Bao, T.-T. Lim, R. Wang, R.D. Webster, X. Hu, Urea-assisted one-step synthesis of cobalt ferrite impregnated ceramic membrane for sulfamethoxazole degradation via peroxymonosulfate activation, Chem. Eng. J. 343 (2018) 737–747. https://doi.org/10.1016/j.cej.2018.03.010.

[22] C. Chu, J. Yang, X. Zhou, D. Huang, H. Qi, S. Weon, J. Li, M. Elimelech, A. Wang, J.-H. Kim, Cobalt Single Atoms on Tetrapyridomacrocyclic Support for Efficient Peroxymonosulfate Activation, Environ. Sci. Technol. 55 (2021) 1242–1250. https://doi.org/10.1021/acs.est.0c06086.

[23] Y. Bao, Y.S. Tay, T.-T. Lim, R. Wang, R.D. Webster, X. Hu, Polyacrylonitrile (PAN)-induced carbon membrane with in-situ encapsulated cobalt crystal for hybrid peroxymonosulfate oxidation-filtration process: Preparation, characterization and performance evaluation, Chem. Eng. J. 373 (2019) 425–436. https://doi.org/10.1016/j.cej.2019.05.058.